PROCEEDINGS OF SCIENCE

Lepto-hadronic inhomogeneous models for AGNs

Gustavo E. Romero
Instituto Argentino de Radioastronomía (IAR-CONICET)
C.C. N° 5, C.P. 1894, Villa Elisa, Buenos Aires, Argentina
Facultad de Ciencias Astronómicas y Geofísicas (FCAG, UNLP)
Paseo del Bosque s/n, La Plata, Buenos Aires, Argentina
E-mail: romero@iar-conicet.gov.ar

I outline the basics of a lepto-hadronic inhomogeneous jet model for the non-thermal broadband emission of radio galaxies and Active Galactic Nuclei (AGNs). I calculate the contribution of relativistic particles, primary electrons and protons as well as secondary muons, charged pions and electron-positron pairs, to the electromagnetic spectrum of the sources. The distribution in energy of all particle species is obtained for an extended, inhomogeneous region. I include detailed analysis of particle energy losses, injection, decay and escape from the acceleration zone and I also calculate absorption effects due to photon-photon annihilation. As an application, I consider the well-known FR I radio galaxy Centaurus A, a nearby source detected by high-energy instruments and suspected to be a cosmic radio source.

AGN Physics in the CTA Era
May 16-17, 2011
Toulouse, France

PoS(AGN 2011)008

1. Introduction

Active Galactic Nuclei (AGNs) can produce radiation along most of the electromagnetic spectrum. In the case of blazars and some nearby Faranhof-Riley Type I radio galaxies, gamma-ray emission has been detected up to TeV energies. To model this emission is a challenge to the current understanding of the physical mechanisms operating in these sources, not only because of the huge energy budget and the complexities of the spectra, but also because of the very rapid variability observed in some sources. This latter fact constraints the emitting region to be located in a small region, likely in the relativistic jets present in all radio loud sources.

The usual approach to deal with the AGN non-thermal emission is to consider the sudden injection of a population of primary relativistic particles (either electron or protons) in a small, homogeneous region of the jet, close to the central supermassive black hole (e.g. Bötcher 2007, Sikora 2011). The physical conditions in the inner jets are, however, likely far from homogeneous, and the acceleration mechanism (e.g. diffusive shock acceleration, magnetic reconnection, or shear accelerations – see Rieger et al. 2007) is likely to operate on both charged leptons and hadrons. Hence, more complex models should be explored.

Here , I outline an inhomogeneous model that takes into account both primary electrons and protons, their transport, the production of secondary and tertiary particles, the transport of these locally generated particles, and all relevant processes leading to non-thermal radiation and its absorption and re-emission. The model is developed from previous work done by Romero & Vila (2008), Reynoso & Romero (2009), and Vila & Romero (2010). It is discussed in full detail by Reynoso et al. (2011). I will show results of the application of such a model to explain a broadband set of data from Centaurus A, the nearest radio galaxy, which has been suggested to be a cosmic ray accelerator long ago (e.g. Romero et a1. 1996), and recently detected by *Fermi* gamma-ray satellite and other instruments (Abdo et al. 2009).

2. Jet model

The model described here is presented in detail in Reynoso, Medina, & Romero (2011). Two symmetrical jets are injected at a distance $z_0 = 50R_g$ from a black hole of mass $M_{\rm BH}$; $R_g = GM_{\rm BH}/c^2$ is the gravitational radius of the black hole. The outflow advances with a bulk Lorentz factor $\Gamma_{\rm jet}$, expanding laterally as a cone of half-opening angle $\phi_{\rm jet}$. I assume that the radiative part of the jet terminates at $z = z_{\rm end}$. The angle between the jet axis and the line of sight is θ.

The accretion power of the black hole is taken as a fraction of the associated Eddington luminosity, $L_{\rm accr} = q_{\rm accr}L_{\rm Edd}$. Following the disk-jet coupling hypothesis of Falcke & Biermann (1995), I assume that a fraction of the accretion energy powers the jets: $2L_{\rm jet} = q_{\rm jet}L_{\rm accr}$, with $q_{\rm jet} \sim 0.1$. The factor 2 takes into account the existence of a jet and a counterjet.

The mean value of the magnetic field at the jet injection point, $B_0 \equiv B(z_0)$, is determined demanding equipartition between the magnetic and kinetic energy densities. For larger z I parameterize the magnetic field as a power law, $B(z) = B_0(z_0/z)^m$, with $1 \leq m \leq 2$.

Part of the jet power is converted into kinetic energy of relativistic particles through a diffusive shock acceleration mechanism in a region where the magnetic energy has drop to values such as the fluid is compressible by internal plasma collisions. The power injected in relativistic particles

is $L_{\rm rel} = q_{\rm rel} L_{\rm jet}$. Both protons and electrons are accelerated, so $L_{\rm rel} = L_e + L_p$ where L_p and L_e are the power injected in relativistic protons and electrons, respectively. These two quantities relate as $L_p = aL_e$, with $a \geq 1$ a free parameter.

The acceleration region is located at $z_{\rm acc} > z_0$. The value of $z_{\rm acc}$ is such that the magnetic energy density is smaller that the jet kinetic energy density at that distance from the black hole (see Komissarov et al. 2007 for a discussion on this topic). The injection function of relativistic primary protons and electrons is assumed to be of the form

$$Q(E,z) = Q_0\, f(z)\, E^{-\alpha} \exp\left(-\frac{E}{E_{\rm max}}\right) \qquad [Q] = {\rm erg}^{-1}\,{\rm cm}^{-3}\,{\rm s}^{-1}. \tag{2.1}$$

Here $E_{\rm max}(z)$ is the maximum energy that particles can achieve at fixed z; it is determined by the balance of the total energy loss rate and the acceleration rate (see below). The function $f(z)$ is given by a step-like function, that is unity for $z \lesssim z_{\rm max}$ and becomes negligible for larger z.

Neutral and charged pions are created through the interaction of relativistic protons with photons and non-relativistic protons. Whereas neutral pions decay into photons, charged pions yield neutrinos, muons and electrons/positrons; muons in turn decay into neutrinos and electrons/positrons. Electron/positron pairs are also directly injected in proton-photon collisions. For a complete list of expressions regarding the injection functions of secondary particles, see Reynoso & Romero (2009), Romero & Vila (2008) and references therein.

The isotropic steady-state energy distribution of relativistic primary and secondary particles in the jet co-moving reference frame, $N(E,z)$ (${\rm erg}^{-1}\,{\rm cm}^{-3}$), is calculated solving the transport equation (Khangulyan et al. 2008)

$$\frac{\partial N}{\partial t} + v_{\rm conv}\frac{\partial N}{\partial z} + \frac{\partial}{\partial E}\left(\frac{dE}{dt}N\right) + \frac{N}{T_{\rm dec}} = Q(E,z). \tag{2.2}$$

This equation takes into account particle injection, convection, energy losses and removal of particles due to decay. The convective term $v_{\rm conv}\partial N/\partial z$, where $v_{\rm conv} \sim v_{\rm jet}$ is the particle convection velocity, allows to incorporate the effect of the variation with z of the parameters that characterize the acceleration region. This is not accounted for in one-zone models where the acceleration/emission region is assumed to be homogeneous, or at least thin enough to neglect all spatial dependence. The decay term is non-zero only for pions and muons. In case of very relativistic bulk motions corrections are necessary and the equation can be written as (Webb 1985):

$$\Gamma_{\rm jet}\frac{\partial N}{\partial t} + \frac{\partial[\Gamma_{\rm jet} v_{\rm conv} N]}{\partial z} + \frac{\partial}{\partial E}\left(\frac{dE}{dt}N\right) + \frac{N}{T_{\rm dec}} = Q(E,z). \tag{2.3}$$

I include both adiabatic and radiative energy losses. In the case of leptons (primary electrons, secondary electron/positron pairs and muons) I consider losses due to synchrotron radiation, relativistic Bremsstrahlung and inverse Compton scattering. For protons and pions, I take into account cooling due to synchrotron radiation and inelastic collisions with photons and thermal protons. The synchrotron field of primary electrons is used as target photon field for inverse Compton scattering, proton-photon and pion-photon collisions. External photons fields from the disk and ambient gas are also included in calculations for specific sources with available observational data. Convenient

expressions for the energy loss rates for all these processes can be found in Reynoso et al. (2011), Reynoso & Romero (2009), and Romero & Vila (2008).

The maximum energy of primary protons and electrons at fixed z is determined equating the total energy loss rate with the acceleration rate $dE/dt|_{\rm acc} = \eta\, e\, c\, B(z)$. The acceleration efficiency $\eta < 1$ depends on the physical details of the acceleration mechanism; I simply regard it as a free parameter of the model.

For a given set of values of the model parameters, radiative output due to all the interaction processes mentioned above can be calculated. The correspondent formulas for the photon emissivities and other details about the calculations are presented in Romero & Vila (2008), Reynoso & Romero (2009) and references therein.

Finally, the correction to the primary emission spectrum due to internal photon absorption through pair creation, $\gamma\gamma \to e^+e^-$, is estimated. The opacity $\tau_{\gamma\gamma}$ for this process is calculated as in Gould & Schréder (1966).

3. Application to Centaurus A.

Centaurus A (Cen A) is the nearest active galaxy, located at ~ 3.5 Mpc. A full but not update description can be found in Israel (1998). In order to apply the model to the inner jet of this source I consider the the set of parameters listed on Table 1. The cooling rates for high energy electrons and protons for this configuration are shown in Fig. 1, while the obtained electron and proton distributions $N_e(E,z)$ and $N_p(E,z)$ are presented in Fig. 2.

It can be seen in Fig. 1 that the relevant energy looses are due to synchrotron cooling for electrons and $p\gamma$ interactions for protons. Since the plot corresponds to the injection zone ($z = z_{\rm acc}$), $p\gamma$ interactions are favored by a large density of target photons corresponding to the synchrotron emission of electrons. These photo-hadronic interactions are not so important for protons outside the injection zone.

It is important to notice that the maximum energy achievable for the protons in this context is of 2×10^7 GeV. These protons can not account for the UHE cosmic rays detected by the Pierre Auger Observatory in the direction of Cen A but it gives a hint to other explanations. If neutrons of the same energy are produced by pion photo-production inside the jet, these could been beamed along the jet and decay into protons near the outer radio lobes, where they would be re-accelerated up to the observed energies by Auger.

Fig. 2 shows that the electron distribution drops quickly with z at the end of the injection zone, while the proton distribution is also important further along the jet. This is a consequence of the different energy loss rates of the particles: electrons cool very rapidly emitting synchrotron radiation, and protons lose energy at a much lower rate as they propagate along the jet.

The SED of Cen A (see Fig. 3) includes the HESS spectrum in the VHE range together with data from *Fermi*/LAT, *CGRO*/COMPTEL, *RXTE* and *INTEGRAL*. I also include data from *HST*/NICMOS and WFPC2, SCUBA at 800 μm, ISO and SCUBA (450 μm and 850 μm), *XMM*-Newton, *Chandra*, and *Suzaku*. See Reynoso et al. (2011) for full references. The data set is not from a single epoch.

The *Fermi*/LAT analysis revealed that the high-energy spectrum is non-variable over the first ten months of scientific operation of the instrument. This steady behavior is also supported by the

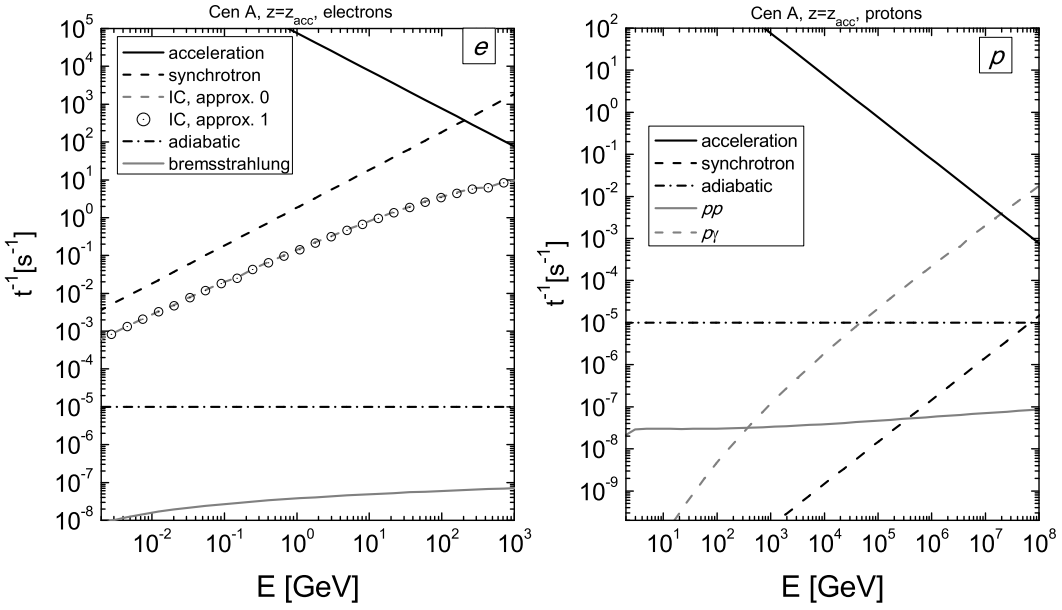

Figure 1: Accelerating and cooling rates for electrons (*left*) and for protons (*right*) at a distance $z = z_{\rm acc}$ from the central engine of Cen A. In the case of electrons, the light-grey dashed line correspond to the first calculation of the IC cooling rate taken into account only synchrotron cooling to obtain the electron distribution. A second approximation to the electron distribution leads to the IC cooling rate indicated in white circles.

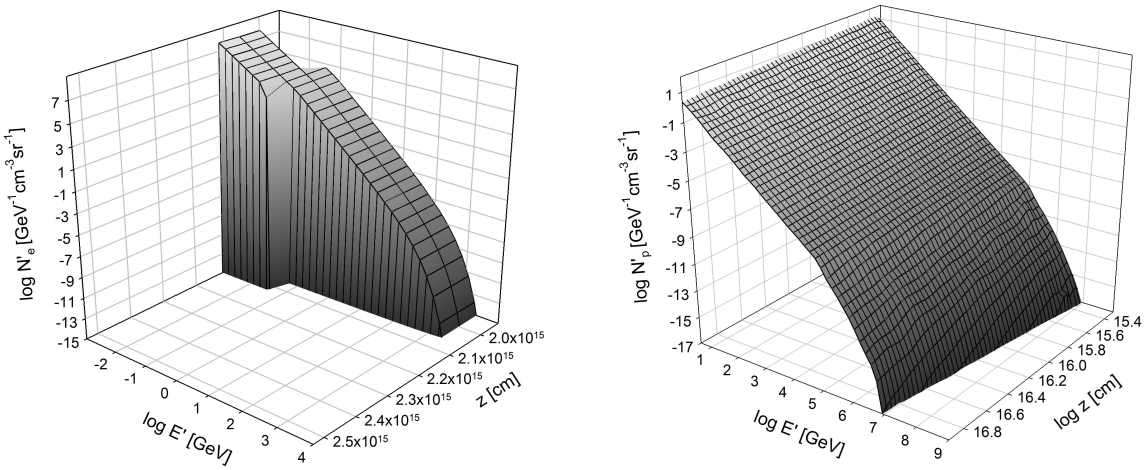

Figure 2: Distributions of primary particles as function of the energy and the distance to the core inside the Cen A jet.*Left*: electrons; *right*: protons.

Table 1: Model parameters for Cen A

Parameter	Value
$M_{\rm bh}$: black hole mass	$10^8 M_\odot$
$R_{\rm g}$: gravitational radius	1.47×10^{13}cm
$L_{\rm jet}^{\rm (kin)}$: jet kinetic power at z_0	6.28×10^{44}erg s^{-1}
$q_{\rm jet}$: ratio $2L_{\rm jet}^{\rm (kin)}/L_{\rm Edd}$	0.1
$\Gamma_{\rm jet}(z_0)$: bulk Lorentz factor of the jet at z_0	3
θ: viewing angle	30°
$\xi_{\rm jet}$: jet's half-opening angle	2.5°
$q_{\rm rel}$: jet's content of relativistic particles	0.05
a: hadron-to-lepton power ratio	0.025
z_0: jet's launching point	50 $R_{\rm g}$
$q_{\rm m}$: magnetic to kinetic energy ratio at $z_{\rm acc}$	0.38
$z_{\rm acc}$: injection point	$132\,R_{\rm g}$
Δz: size of injection zone	$2\,z_{\rm acc}\tan\xi_{\rm jet} = 11.5\ R_{\rm g}$
$B(z_{\rm acc})$: magnetic field at $z_{\rm acc}$	3065 G
m: index for magnetic field dependence on z	1.5
s: injection spectral index	1.8
η: acceleration efficiency	10^{-2}
$E_p^{\rm (min)}$: minimum proton energy	3 GeV
$E_e^{\rm (min)}$: minimum electron energy	0.1 GeV
$E_p^{\rm (max)}$: maximum primary proton energy	2×10^7 GeV
$E_e^{\rm (max)}$: maximum primary electron energy	200 GeV
N_H: column dust density	10^{23} cm^{-2}
$n_c(z_{acc})$: cold matter density inside the jet at $z_{\rm acc}$	3×10^8 cm^{-3}

HESS experiment, which also reported a constant flux from Cen A even though *CGRO* data shows some variability with at least two emission states during the period 1991-2000.

Since the set of measurements composing the SED of Cen A is quite inhomogeneous in time and angular resolution, so one should be very careful in attempting to interpret any fit of all the spectrum simultaneously. In particular, the data that define the bump in the hard-X-rays ($\sim$0.1 MeV) have been taken more than 10 years ago with a poor angular resolution and long integration times. The lack of a good spatial resolution makes impossible to distinguish the emission components (jet, nucleus or other radiation sources). Furthermore, I note a discrepancy between the flux normalization of *Fermi*/LAT and HESS, which is not yet fully understood.

Nevertheless, the application of the model yields a spectral energy distribution which is basically consistent with the multi-wavelength emission from Cen A.

An important role is played by absorption due to photoionization interactions in the sur-

rounding dust. This arises due to the large value of the column density of neutral hydrogen, $N_H = 10^{23}\mathrm{cm}^{-2}$. A drastic modulation is then imprinted in the electron synchrotron spectrum, which is responsible for the whole emission in the broadband range $10^{-5} - 10^{7}$eV. Such situation is possible if electrons can be efficiently accelerated ($\eta = 0.01$) to high energies with a rather flat spectral index ($s = 1.8$). The internal $\gamma\gamma$ absorption does not modify significantly the pp contribution of gamma-rays, since it is only important within the injection zone, which is a negligible region of the jet compared to the one in which pp collisions occur (see Fig. 2).

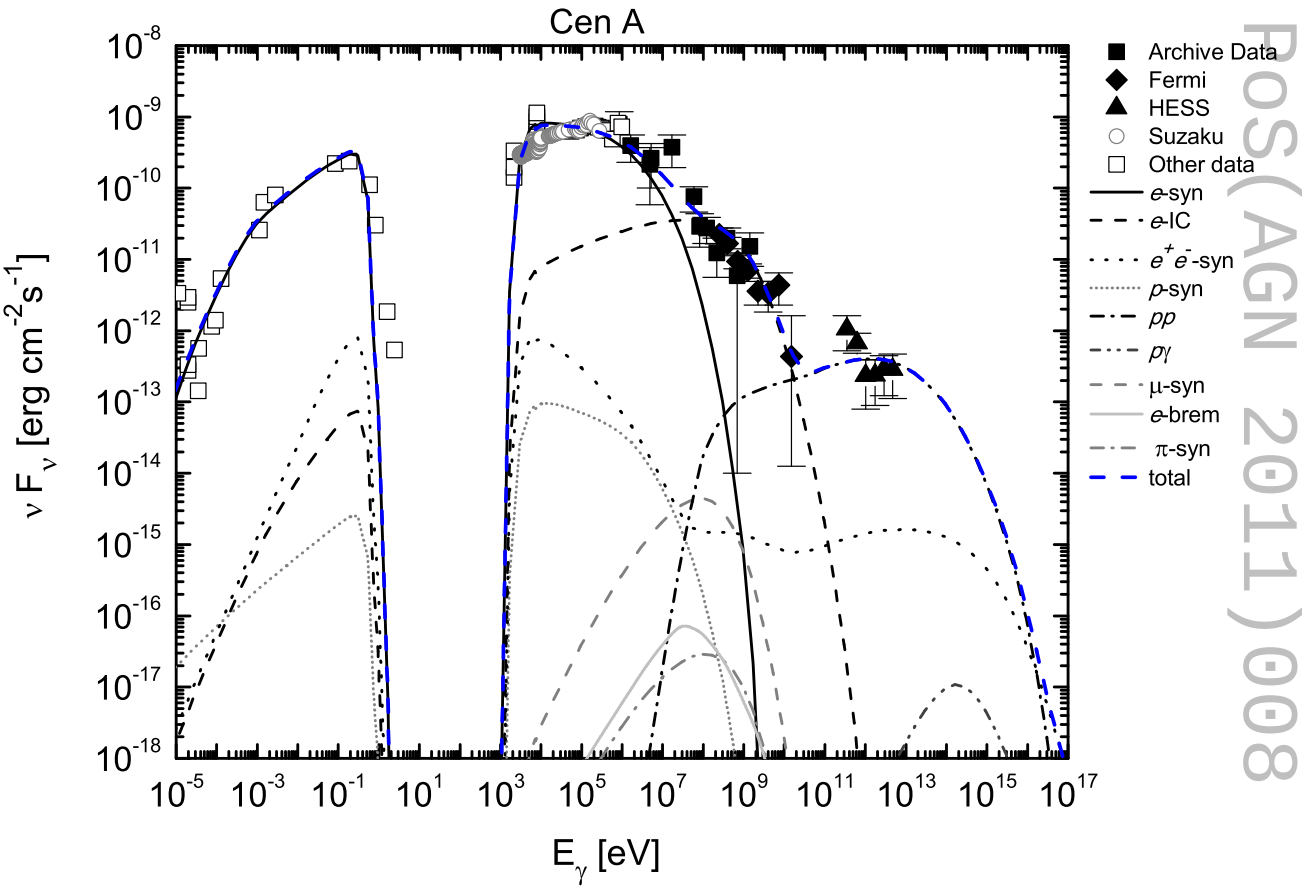

Figure 3: Model output for the SED of Cen A. The different emission processes are indicated, together with the total output. The recent observational data is also included: *Fermi*/LAT (black filled diamons) and HESS spectra (black filled triangles). The rest of the data points correspond to instruments mentioned in the text.

I evaluate the accompanying neutrino output using the same set of parameters. The obtained differential flux, weighted by the squared energy is plotted in Fig. 3 together with the estimated sensitivity of KM3Net for one year of operation. It can be seen in this figure that the neutrino signal produced by pp and $p\gamma$ interactions would not be observable by KM3NeT detector in just one year of observation. It is to be noticed, however, that the sensitivity level shown in the plot actually corresponds to a neutrino spectrum with an E_ν^{-2} dependence, which is a bit steeper than in the present case. Hence, it can be expected that the actual sensitivity for the flux will be better than what is shown here, so with two or three years of data taking it would be possible to achieve

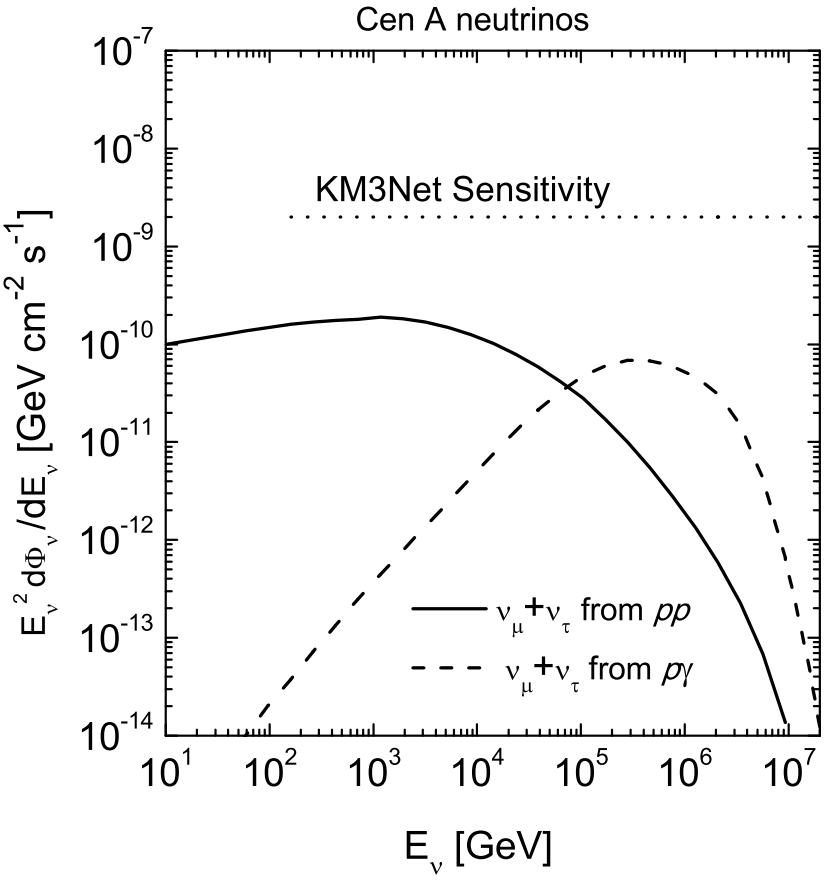

Figure 4: Differential neutrino flux weighted by the squared energy as predicted by the model for Cen A. *Dotted line*: Approximate KM3Net sensitivity for 1 year operation.

detection.

4. Conclusions

I have presented a model for the broadband spectrum of the inner jets of AGNs that includes the radiative contribution of electrons, protons and secondary particles generated by several interaction processes. The energy distributions of all species were obtained solving the transport equation in an inhomogeneous region, taking into account cooling, injection, convection and decay. I also assessed the effect of photon absorption in the jet. The model was applied to fit the observed spectrum of the FR I radio galaxy Cenaturus A. Rapid variability can be introduced in the model through shock interactions with small inhomogeneous regions generated by Kelvin-Helmholtz instabilities (Romero 1995). This will be developed in detail in a forthcoming paper.

Acknowledgments

I thank M. Reynoso, Clementina Medina, and Gaby Vila for insightful discussion and help. This work was supported by CONICET grant PIP 0078, by and the Spanish Ministerio de Ciencia e Innovación (MINCINN) under grant AYA 2010-21782-C03-01.

References

[1] A.A. Abdo, M. Ackermann, M., Ajello, et al., *Fermi Large Area Telescope view of the core of the radio galaxy Centaurus A, ApJ* **700** (597) 2009

[2] M. Böttcher *Modeling the emission processes in blazares, Astrophys. Space Sci* **309** (95) 2007

[3] H. Falcke, P.L. Biermann, *The jet-disk symbiosis. I. Radio to X-ray emission models for quasars, A&A* **293** (665) 1995

[4] R.J. Gould, G. Schréder, *Opacity of the Universe to High-Energy Photons, Phys. Rev. Lett.* **16** (6) 1966

[5] F.P. Israel, *Centaurus A - NGC 5128, A&ARv* **8** (237) 1998

[6] S. Komissarov, M. Barkov, N. Vlahakis, A. Königl, *Magnetic acceleration of relativistic active galactic nucleus jets, MNRAS* **380** (1) 2007

[7] D. Khangulyan, F. Aharonian, V. Bosch-Ramon, *On the formation of TeV radiation in LS 5039, MNRAS* **383** (467) 2008

[8] M.M. Reynoso, G.E. Romero, *Magnetic field effects on neutrino production in microquasars, A&A* **531** id. 30, 2011

[9] M.M. Reynoso, M.C. Medina, G.E. Romero, G.E. *A lepto-hadronic model for high-energy emission from FR I radiogalaxies, A&A* **493** (1) 2009

[10] F.M. Rieger, V. Bosch-Ramon, P. Duffy *Fermi acceleration in astrophysical jets, Astrophys. Space Sci* **309** (1191) 2007

[11] G.E. Romero, *Fine-scale structure in relativistic jets and rapid variability in blazars, Astrophys. Space Sci* **234** (49) 1995

[12] G.E. Romero, J.A. Combi, S.E. Perez Bergliaffa, L.A. Anchordoqui, *Cenaturus A as a source of cosmic rays well beyond the GZK cutoff, Astroparticle Physics*,**5** (279) 1996

[13] G.E. Romero, G.S. Vila, *The proton low-mass microquasar: high-energy emission, A&A* **485** (3) 2008

[14] M. Sikora, *Hadronic jet models today, IAU Symp.* **275** (59) 2011

[15] G.S. Vila, G.E. Romero *Leptonic/hadronic models for electromagnetic emission in microquasars: the case of GX 339-4, MNRAS* **403** (1457) 2010

[16] G.M. Webb, *Relativistic transport theory for cosmic rays, ApJ* **296** (319) 1985